J. Chem. Eng. Data **1991**, *36*, 265-268

Binary Gaseous Diffusion Coefficients of Mercury and of Zinc in Hydrogen, Helium, Argon, Nitrogen, and Carbon Dioxide

Peter J. Gardner,* Peter Pang, and Steve R. Preston

Department of Chemistry, Royal Holloway and Bedford New College, University of London, Egham Hill, Egham, Surrey TW20 0EX, U.K.

Binary gaseous diffusion coefficients at 1 atm of pressure for Zn and for Hg with H_2, He, Ar, N_2, and CO_2 have been determined in the ranges 420–590 K (for Hg) and 690–1140 K (for Zn) by using the modified entrainment method. The results are interpreted in terms of two intermolecular potentials.

Introduction

This paper describes the determination of binary gaseous diffusion coefficients from 420 to 1140 K for Hg and for Zn with some inert gases and simple polyatomic species. Given the nature of the interacting systems, nonpolar, monoatomic, or simple polyatomic, the Lennard-Jones (12,6) potential was surprisingly inadequate in the interpretation of the experimental results, probably because of the inflexibility in the form of the repulsive core. Another potential function, the $n(\bar{r})$-6 potential of Maitland and Smith (*1*) was more flexible in this respect and was parametrized to the systems studied with enhanced agreement.

Experimental Section

The modified entrainment method has been described in detail (*2*–*4*). The current apparatus was closely modeled on the original design (*2*), and various improvements to the gas handling system, etc., have been described (*3*, *4*). A significant improvement to the capsule design was used for the first time in this work in that the channel was inset by ≈5 mm into the capsule (see below); this means the channel dimensions may be defined more precisely. Briefly, the sample (liquid zinc or mercury in these experiments) was contained in a spherical silica capsule, the orifice of which is a narrow reentrant channel of known geometry (ca. 20-mm length × 1-mm i.d.). The channel resistances (length over cross-sectional area) were determined by measuring the channel lengths with a traveling microscope and measuring the mean channel radii by filling the channel with mercury and weighing; they were 2.132×10^4 m^{-1} for the Zn and 2.114×10^4 m^{-1} for the Hg experiments. The capsule is suspended by a silica fibre from a Cahn R100 electrobalance, so that the mass loss may be measured continuously. The capsule was positioned at the center of a temperature plateau of a vertically mounted tube furnace. The carrier gas flow is directed axially over the channel orifice so that the emergent gas concentration at this point is effectively zero. The maximum local volume fractions of Hg or Zn in the vicinity of the open end of the channel may be calculated from the appropriate fluxes at the highest experimental temperatures and the flow rate of the carrier gas; these maxima are 0.012 for Zn and 0.004 for Hg. The flow rates used and the equipment geometry are such that the drag factor is insignificant and constant; the effect of flow rate on the rate of mass loss has been described (*2*). The drag was measured at 300 and 505 K with a range of nitrogen flow rates. Extrapolating these results to higher temperatures, the resultant drag at a 90 cm^3 (STP) min^{-1} carrier gas flow rate expressed as a fraction of capsule mass was 0.01% (at 505 K) and 0.02% (at 970 K); the variation arises from changing viscosity and buoyancy effects with temperature.

A calibrated NiCr/NiAl thermocouple was positioned directly underneath the capsule for the experiments with Hg and a Pt/(Pt + 13% Rh) thermocouple was similarly positioned for the experiments with Zn. This second thermocouple was calibrated in situ, and the radiation correction for the NiCr/NiAl thermocouple, used below 590 K, was judged negligible. Temperature was measured to ±1 K, and experimental values of the rate of mass loss varied between 10^{-12} and 10^{-8} kg s^{-1}. The downward flow of carrier gas was kept at a constant flow rate of 90 cm^3 (STP) min^{-1} by an ASM mass flow controller. The method is a modification of the capillary leak, or evaporation tube, method pioneered by Stefan (*5*). The apparatus has been tested with a system of known diffusivity (*3*).

Materials. Triply distilled mercury and 0.27-mm-diameter zinc wire (Goodfellow Metals Ltd., 99.99+%) were used to generate the common gases in this work. The hydrogen carrier gas (high purity grade, BOC, 99.99+%) was further purified by passing it through a palladium diffuser (Johnson Matthey, Model H28/1). Argon (high purity grade, BOC, 99.999+%), helium (CP grade, BOC, 99.999+%), nitrogen (oxygen-free grade, BOC, 99.9+%) were dried by passing them through columns containing activated 4-Å molecular sieves. The argon and helium were further purified by passage through a rare gas purifier (Model RGP-4, BOC).

Results

If the capsule contains a single substance, then the experimental rate of weight loss ($\dot{w}$) is a simple function of the saturated vapor pressure of that single substance (p°_1), the temperature (T), the diffusive resistance of the channel (l/A, length over cross-sectional area), and the binary diffusion coefficient (D_{12})

$$p^\circ_1 = P(1 - e^{-\xi}) \tag{1}$$

where

$$\xi = \dot{w}RTl/D_{12}AM_1P \tag{2}$$

and where M_1 is the atomic mass of zinc or mercury and P is the operating pressure (atmospheric pressure plus 3–4 mmHg). The vapor pressures of zinc (liquid) and mercury are known over a wide range of temperature so D_{12} can be obtained by rearrangement of the above equations.

The transport of gaseous mercury and zinc in several different carrier gases was studied in the range 424–590 K for mercury (T_b = 630 K) and in the range 820–1140 K for zinc (T_m = 629.6 K, T_b = 1186 K). The vapor pressure equations for liquid mercury and zinc are given by Ambrose and Sprake (*6*) and Nesmeyanov (7), respectively.

$$\log_{10}(p^\circ_{Hg}/\text{kPa}) = 7.65879 - \frac{3279.23}{T} - 9.6803 \times 10^{-4}T + 4.11546 \times 10^{-7}T^2 \tag{3}$$

$$\log_{10}(p^\circ_{Zn}/\text{Pa}) = -5.7941 - \frac{5330.735}{T} - 0.00161644T + 5.59972 \log_{10} T \tag{4}$$

The temperature dependence of the diffusion coefficients was accommodated by fitting the experimental results to $D_{12} = D_0(T/T_0)^{1+s}$, where the reference temperature, T_0, was

0021-9568/91/1736-0265$02.50/0

Table I. Experimental Temperatures and Mean Diffusion Coefficients Compared with Values Calculated Assuming Maitland–Smith (MS) and Lennard-Jones (LJ) Potentials

system	T/K	n^a	$10^4\langle D\rangle$/ ($m^2\ s^{-1}$)	10^4D(MS)/ ($m^2\ s^{-1}$)	10^4D-(LJ)/($m^2\ s^{-1}$)
Hg–H_2	421.2	2	1.13	1.23	1.26
	429.2	10	1.19	1.27	1.30
	450.2	6	1.29	1.38	1.42
	469.2	4	1.39	1.49	1.53
	480.2	4	1.41	1.55	1.60
	510.2	5	1.61	1.73	1.78
	539.2	6	1.66	1.91	1.97
	569.2	10	1.86	2.10	2.17
	589.2	10	1.91	2.23	2.31
Hg–He	430.2	8	1.12	1.22	1.30
	448.7	7	1.18	1.31	1.40
	468.7	6	1.28	1.42	1.50
	497.2	7	1.37	1.57	1.66
	507.2	5	1.48	1.62	1.72
	527.7	5	1.54	1.74	1.84
	546.2	4	1.63	1.84	1.95
	565.2	5	1.74	1.96	2.06
Hg–N_2	429.2	5	0.273	0.263	0.264
	450.2	7	0.302	0.288	0.288
	479.2	4	0.340	0.325	0.323
	509.2	6	0.378	0.364	0.361
	519.2	9	0.396	0.378	0.374
	540.2	6	0.410	0.407	0.402
	570.2	6	0.455	0.451	0.444
	590.2	5	0.482	0.481	0.472
Hg–Ar	449.2	3	0.235	0.241	0.253
	479.2	3	0.267	0.273	0.286
	508.2	10	0.295	0.305	0.319
	525.2	6	0.309	0.325	0.339
	538.2	8	0.318	0.340	0.355
	569.2	5	0.348	0.377	0.393
	590.2	11	0.368	0.404	0.420
Hg–CO_2	431.2	7	0.234	0.220	0.171
	451.7	4	0.238	0.241	0.187
	471.2	4	0.241	0.261	0.203
	491.2	5	0.283	0.283	0.220
	501.2	7	0.284	0.295	0.229
	533.2	6	0.313	0.332	0.258
	551.2	6	0.324	0.354	0.275
	573.2	6	0.350	0.382	0.296
Zn–H_2	780.1	3	4.08	3.70	4.53
	818.2	3	4.37	4.02	4.94
	847.9	4	4.73	4.28	5.26
	907.9	3	5.18	4.83	5.93
	946.5	5	5.47	5.20	6.38
	977.4	6	5.74	5.51	6.75
	998.9	7	5.93	5.72	7.01
	1031.6	5	6.22	6.06	7.42
	1052.8	5	6.45	6.28	7.69
	1084.8	6	6.81	6.62	8.10
	1117.9	5	7.18	6.97	8.53
Zn–He	828.8	2	3.53	3.99	4.94
	858.8	4	3.70	4.25	5.25
	887.5	3	3.95	4.50	5.54
	916.6	6	4.16	4.76	5.85
	946.3	5	4.32	5.04	6.18
	977.4	5	4.62	5.33	6.52
	1009.4	5	4.84	5.65	6.88
	1042.1	4	5.12	5.97	7.26
	1074.5	3	5.36	6.30	7.64
	1117.8	6	5.72	6.76	8.16
Zn–N_2	800.9	1	1.13	0.924	1.03
	848.9	10	1.28	1.03	1.15
	878.1	9	1.33	1.10	1.22
	897.3	4	1.39	1.14	1.27
	927.5	7	1.44	1.21	1.34
	957.4	11	1.51	1.28	1.42
	989.2	3	1.58	1.36	1.50
	1031.3	6	1.69	1.47	1.62
	1073.9	7	1.82	1.58	1.74
	1107.2	8	1.97	1.67	1.83
	1135.0	6	2.15	1.75	1.91
Zn–Ar	819.5	1	0.930	0.837	1.00
	859.4	3	0.982	0.914	1.09
	872.6	3	1.03	0.940	1.12
	887.6	2	0.917	0.970	1.16
	917.3	4	1.12	1.03	1.23
	955.9	2	1.17	1.11	1.32
	989.0	3	1.23	1.18	1.41
	1031.6	4	1.34	1.28	1.51
	1064.0	6	1.43	1.35	1.60
	1096.6	5	1.50	1.43	1.69
	1119.0	5	1.58	1.48	1.75
	1140.4	5	1.61	1.53	1.81

[a] n is the number of experimental values of D averaged at any given temperature.

chosen as 273.15 K. The inverse pressure dependence of the diffusion coefficient could also be included in this equation, but the small fluctuations in atmospheric pressure occurring during the course of the experiments caused changes in D_{12} that were within the random scatter of the results. The mean results at each temperature are shown in Table I; they are compared with calculated values at the same temperatures obtained assuming two separate intermolecular potentials (see Discussion). Values for D_0 and $1 + s$ were obtained by linear regression and are collected in Table II. Figure 1 is a plot of D_{12} vs T for some of the mercury systems with error limits shown for the experimental data and the regression line calculated from the coefficients in Table II superimposed.

Table II. Constants for the Equation $D_{12} = D_0(T/T_0)^{1+s}$ Obtained by Linear Regression (T_0 = 273.15 K)

$system^a$	10^5D_0/($m^2\ s^{-1}$)	$1 + s$	temp/K
Hg–H_2	5.962 ± 0.081^b	1.535 ± 0.022^b	421–589
Hg–He	5.320 ± 0.073	1.619 ± 0.023	430–586
Hg–N_2	1.252 ± 0.023	1.761 ± 0.029	429–590
Hg–Ar	1.099 ± 0.021	1.573 ± 0.029	429–590
Hg–CO_2	1.072 ± 0.032	1.594 ± 0.049	430–590
Zn–H_2	8.167 ± 0.214	1.534 ± 0.021	690–1118
Zn–He	5.743 ± 0.085	1.632 ± 0.012	829–1118
Zn–N_2	1.879 ± 0.090	1.673 ± 0.038	800–1135
Zn–Ar	1.242 ± 0.094	1.793 ± 0.058	820–1140

[a] The mole fraction range of the common gas in the carrier was 0.005–0.46 for Hg systems and 0.0002–0.63 for Zn systems. [b] The uncertainty intervals are ±1 sd of the regression coefficients.

Discussion

In this section we compare our experimental results with values calculated by assuming two separate intermolecular potentials. Binary gaseous diffusion coefficients may be readily calculated in the dilute gas limit from the Chapman–Enskog (*8*) equation. This equation requires a collision integral that is temperature-dependent and is evaluated for a specific analytical form of intermolecular potential. Reid et al. (9) assume a Lennard-Jones potential and tabulate results of calculations for 114 gas pairs, noting a mean absolute deviation from the experimental values of 7.5%. This calculation was repeated for our systems by using the Lennard-Jones molecular parameters recommended by Reid et al. (*9*) that were obtained from the inversion of viscosity data by Svehla (*10*). There are more recent (*11*, *12*) collections of the Lennard-Jones (LJ) parame-

Table III. Molecular Parameters for the $n(\bar{r})$–6 Potential and Comparison of Calculated and Experimental Diffusion Coefficients[a]

system	T*[b]	σ_2[c]/Å	ϵ_2/k_B[c]/K	σ_{12}/Å	ϵ_{12}/k_B/K	γ_2	m_2	Δ[d](LJ[e])/%	$10^5 D_0$(MS)/($m^2\ s^{-1}$)	1 + s(MS)	Δ[d](MS)/%
Hg–H_2	3–4	3.08_5	33.2	3.16	144	−3.7	8.3	−14	5.676	1.783	−11
Hg–He[f]	5–7	2.633	10.9	2.93	83	6.0	12	−18	5.573	1.727	−12
Hg–N_2	1.4–1.9	3.22	154.9	3.22	312	7.6	13	+4	1.118	1.896	+3
Hg–Ar[g]	1.4–2.0	3.35	141.5	3.29	298	7.5	13	−9	0.944	1.888	−4
Hg–CO_2	1.2–1.7	3.04	200	3.13	354	10.4	11.3	+18	0.909	1.936	5*
Zn–H_2	5–8	3.08_5	33.2	3.24	143	−3.7	8.3	−15	5.776	1.768	+6
Zn–He	10–14	2.633	10.9	3.02	82	6.0	12	−42	5.632	1.764	−16
Zn–N_2	2.6–3.7	3.22	154.9	3.31	309	7.6	13	+7	1.292	1.830	+16
Zn–Ar[h]	2.8–3.9	3.35	141.5	3.38	295	7.5	13	−12	1.113	1.821	6*

[a] For Hg systems, σ, ϵ/k_B, γ, and m equal 3.23 Å, 627 K, 10.8, and 11.5, respectively. For Zn systems, σ, ϵ/k_B, γ, and m equal 3.4 Å, 615 K, 8.9, 6.2, respectively. [b] $T^* = k_B T/\epsilon$. [c] Potential parameters for He and Ar are taken from Table 8.2 of ref 12; the derivation of the remainder is described in the text. Species 1 is Hg or Zn. [d] $\Delta = 100(D(\text{exp}) - D(\text{calc}))/D(\text{exp})$ and is the mean value of Δ calculated at 5 K intervals in the experimental temperature range. If the deviation changes sign in this range, the mean *absolute* deviation is quoted (indicated with an asterisk); LJ = Lennard-Jones potential, MS = Maitland–Smith or $n(\bar{r})$-6 potential (*1*). [e] The LJ potential parameters were taken from ref 9; no value for Zn is given, and an empirical correlation of Svehla (*10*) was used to estimate the following for Zn systems: $\sigma \approx 2.28$ Å; $\epsilon/k_B \approx 1393$ K. The Neufeld et al. (*30*) analytic expression for the reduced collision integral was used. [f] From the electronic spectrum of the van der Waals complex, for the Hg–He system, σ and ϵ/k_B equal 4.07 Å and 11, respectively, (*28*). [g] From the electronic spectrum of HgAr, ϵ/k_B = 204 (*26*); ab initio calculations (*27*) are in good agreement. [h] From the electronic spectrum of ZnAr, σ and ϵ/k_B equal 3.64 Å and 138, respectively, (*29*).

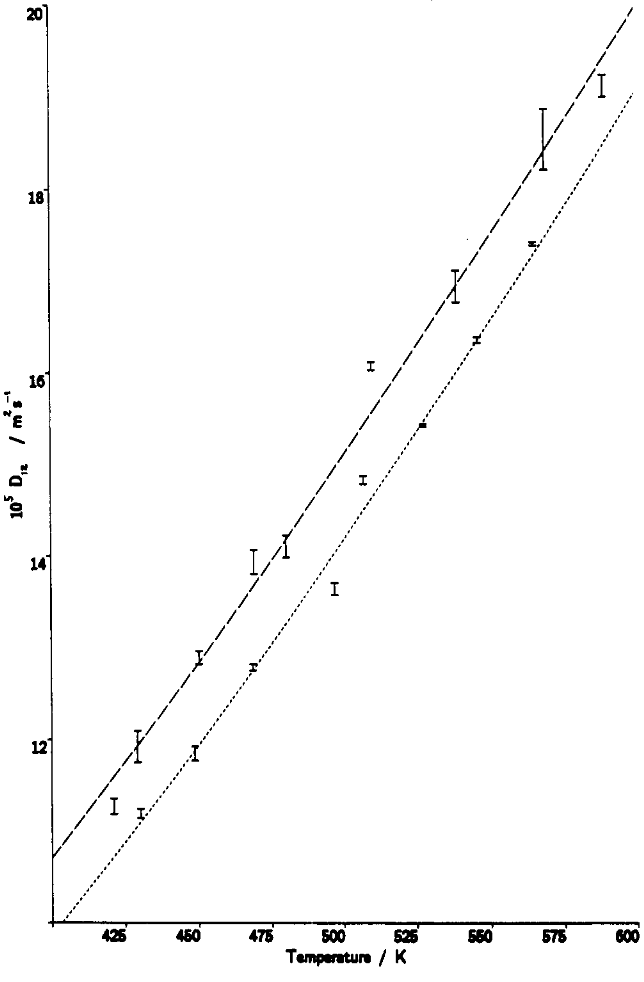

Figure 1. Temperature variation for D(Hg–H_2) (– –) and D(Hg–He) (···). The error bars indicate the uncertainty in the experimental results, and the broken lines are regression lines plotted by using the coefficients in Table II.

ters (not including Hg, Zn, or H_2, however), but it is well established (*11*, *13*, *14*) that there is strong cross-correlation between ϵ and σ and hence there appears to be little merit in using incomplete or mixed data sets.

From the results given in Table III, it is apparent that there is extremely poor agreement between the experimental results and data calculated assuming an LJ potential; the differences range from −42 to +18%, and only the systems containing N_2 show agreement approaching the mean precision of Reid et al. (*9*). It is well-known (*15*) that concentration effects, ignored in a first-order treatment, are significant when the masses of the interdiffusing species are widely disparate. However, when the majority component is the lighter, these effects are usually insignificant. Calculation including second-order concentration-dependent terms for the Hg–H_2 system at a mole fraction of 0.46 (the maximum experimental concentration of Hg, see Table II) yielded a value of 1.1% in excess of the result from the corresponding first-order calculation; it seems unlikely therefore that neglect of these terms is responsible for the differences noted in Table III. There is evidence (*16*, *17*) from molecular beam studies that the Lennard-Jones intermolecular potential is quite inadequate for both the Hg–H_2 and Hg–He systems.

A simple potential that accurately reproduces the potential functions for the inert gas pairs is the $n(\bar{r})$-6 function (*1*) of Maitland and Smith (MS)

$$U(r) = \epsilon\left(\frac{6}{n-6}\left(\frac{r_m}{r}\right)^n - \frac{n}{n-6}\left(\frac{r_m}{r}\right)^6\right) \tag{5}$$

where

$$n = m + \gamma\left(\frac{r}{r_m} - 1\right) \tag{6}$$

In these equations, ϵ is the well depth, r_m is the separation at $U = \epsilon$, and m and γ are constants. The advantage of this potential compared to the LJ potential (to which it reduces with $m = 12$ and $\gamma = 0$) is the flexibility imparted to the repulsive limb of the potential function, which is r-dependent. For $r > r_m$, the two forms (LJ and MS) are closely coincident. The experimental results reported here all at $T^*(=k_B T/\epsilon) > 1$, where the attractive component of the intermolecular potential is relatively unimportant.

There are ab initio molecular orbital calculations for both Zn_2 (*18*) and Hg_2 (*19*) and supported by experimental results for Zn_2 (*20*). These studies yield values of the interatomic potential over a wide range of r that were fitted by multivariate regression to eq 5; for inert gas pairs, Rigby et al. (*12*) recommend m = 13 (except for He where m = 12), but *in this work m was taken as a disposable parameter*—see Table III. The polyatomic gases used in this work are less readily parameterized to the $n(\bar{r})$-6 potential, as the form of the potential is dependent on the relative orientation of the internuclear axes of the interacting molecules. For $(H_2)_2$, ab initio calculations (identified as M80 in ref 21) give an isotropic, i.e. angle-averaged, potential that was regressed as described above. For both $(N_2)_2$ and $(CO_2)_2$, isotropic potentials are not available but individual potentials for specific intermolecular configurations, e.g. linear, crossed, parallel, or T-shaped, have been reported (*22*, *23*). Attempts to combine these angle-dependent potentials to give a statistical and Boltzmann-weighted composite potential similar to the isotropic $(H_2)_2$ potential were not successful in that the resultant $n(\bar{r})$-6 potential parameters did not improve the diffusion coefficients. However, using the potential curves for the crossed configuration of both $(N_2)_2$ and $(CO_2)_2$ gave a significant improvement in the calculated diffusion coefficients, and it is these potential paramters that are given in Table III.

The reduced collision integral ($\Omega^{(1,1)*}$) required in the kinetic theory expression (*8*) for the diffusion coefficient was evaluated by using a procedure described by Barker et al. (*24*). Lorentz–Berthelot rules (*12*) were used to evaluate σ_{12} and ϵ_{12}, and, in the absence of specific literature recommendation, arithmetic means were used for γ_{12} and m_{12}. Molecular parameters and diffusion coefficients calculated from the LJ and the $n(\bar{r})$-6 potentials are compared with the experimental values in Table III.

The limited experimental results (*26*–*29*) that are available for well depths and collision diameters for the experimental systems indicate the geometric mean rule for ϵ_{12} overestimates considerably; comparison is made in a footnote to Table III.

The use of the $n(\bar{r})$-6 potential gives a significant improvement for the calculated diffusion coefficients of the Hg-containing systems; the mean absolute deviation for the five gas pairs studied is ≈7%. An improvement for the Zn-containing systems is also apparent, but the mean absolute deviation is still ≈11%.

Acknowledgment

We gratefully acknowledge helpful discussions with Dr. D. Heyes and Prof. K. Singer.

Literature Cited

(1) Maitland, G. C.; Smith, E. B. *Chem. Phys. Lett.* **1973**, *22*, 483.
(2) Battat, D.; Faktor, M. M.; Garrett, I.; Moss, R. H. *J. Chem. Soc., Faraday Trans. 1* **1974**, *70*, 2267.
(3) Finch, A.; Gardner, P. J.; Tarbox, E.; Yardley, S. *J. Chem. Soc., Faraday Trans. 1* **1979**, *75*, 545.
(4) de Largy, B.; Finch, A.; Gardner, P. J.; Kell, N. *J. Chem. Soc., Faraday Trans. 1* **1983**, *79*, 383.
(5) Stefan, J. *Sitzugber. Akad. Wiss. Wien* **1871**, *63*, 63.
(6) Ambrose, D.; Sprake, C. H. *J. Chem. Thermodyn.* **1972**, *4*, 603.
(7) Nesmeyanov, A. N. *The vapour pressure of the chemical elements*; Elsevier: Amsterdam, 1963.
(8) Chapman, S.; Cowling, T. G. *The mathematical theory of non-uniform gases*; Cambridge University Press: London, 1939.
(9) Reid, R. C.; Prausnitz, J. M.; Sherwood, T. K. *The properties of gases and liquids*, 3rd ed.; McGraw-Hill: New York, 1977.
(10) Svehla, R. A. NASA Technical Report R-132; Lewis Research Center: Cleveland, OH, 1962.
(11) Clifford, A. A.; Gray, P.; Platts, N. *J. Chem. Soc., Faraday Trans. 1* **1977**, *73*, 381.
(12) Rigby, M.; Smith, E. B.; Wakeham, W. A.; Maitland, G. C. *The forces between molecules*; Clarendon Press: Oxford, U.K., 1986.
(13) Hu, A. T.; Chappelear, P. S.; Kobayashi, R. *AIChE J.* **1970**, *16*, 259.
(14) Reichenberg, D. *AIChE J.* **1973**, *19*, 854.
(15) Mason, E. A. *J. Chem. Phys.* **1957**, *27*, 782.
(16) Mueller, C. R.; March, R. P. *J. Chem. Phys.* **1963**, *38*, 745.
(17) Knauer, F. *Z. Phys.* **1934**, *90*, 559.
(18) Hay, P. J.; Dunning, T. H.; Raffenetti, R. C. *J. Chem. Phys.* **1976**, *65*, 2679.
(19) Baylis, W. E. *J. Phys. B* **1977**, *10*, L583.
(20) Su, C. H.; Huang, Y.; Brebrick, R. F. *J. Phys. B* **1985**, *18*, 3187.
(21) Buck, U.; Huisken, F.; Kohlhase, A.; Otten, D. *J. Chem. Phys.* **1983**, *78*, 4439.
(22) Ling, M. S. H.; Rigby, M. *Mol. Phys.* **1984**, *51*, 855.
(23) MacRury, T. B.; Steele, W. A.; Berne, B. J. *J. Chem. Phys.* **1976**, *64*, 1288.
(24) Barker, J. A.; Fock, W.; Smith, F. *Phys. Fluids* **1964**, *7*, 897 (a coding for Barker's collision integral routine is given in Appendix 12 of ref 25).
(25) Maitland, G. C.; Rigby, M.; Smith, E. B.; Wakeham, W. A. *Intermolecular forces-their origin and determination*; Clarendon Press: Oxford, U.K., 1981.
(26) Fuke, K.; Saito, T.; Kaya, K. *J. Chem. Phys.* **1984**, *81*, 2591.
(27) Czuchaj, E.; Stoll, H.; Preuss, H. *J. Phys. B* **1987**, *20*, 1487.
(28) Duvel, M. C.; Jouvet, C.; Soep, B. *Chem. Phys. Lett.* **1985**, *115*, 318.
(29) Wallace, I.; Bennett, R. R.; Breckenridge, W. H. *Chem. Phys. Lett.* **1988**, *153*, 127.
(30) Neufield, P. D.; Janzen, A. R.; Aziz, R. A. *J. Chem. Phys.* **1972**, *57*, 1100.

Received for review February 6, 1990. Revised October 8, 1990. Accepted February 13, 1991.